servable spectroscopically. Probably the best
hope of settling the matter lies with calculations

which include directly the effects of coupling with
the continuum, such as those of Altick.[15]

†Research supported in part by the Advanced Research
Projects Agency of the U. S. Department of Defense
under the Strategic Technology Office.

[1]T. Andersen, K. A. Jessen, and G. Sørensen, Phys.
Rev. 188, 76 (1969).

[2]I. Bergström, J. Bromander, R. Buchta, L. Lundin,
and I. Martinson, Phys. Letters 28A, 721 (1969).

[3]J. Bromander, Physica Scripta 4, 61 (1971).

[4]A. W. Weiss, Nucl. Instr. Methods 90, 121 (1970).

[5]M. W. Smith and W. L. Wiese, Astrophys. J. Suppl.
Ser. 23, 103 (1971).

[6]L. Johansson, Arkiv Fysik 23, 119 (1962).

[7]H. G. Berry, J. Bromander, I. Martinson, and R.
Buchta, Physica Scripta 3, 63 (1971).

[8]C. C. J. Roothaan and P. S. Bagus, Methods in
Computational Physics (Academic, New York, 1963),
Vol. 2, p. 47.

[9]P. S. Bagus (private communication).

[10]P. O. Löwdin and H. Shull, Phys. Rev. 101, 1730
(1956).

[11]A. W. Weiss, Phys. Rev. 166, 70 (1968).

[12]D. R. Bates and A. Damgaard, Phil. Trans. Roy.
Soc. London A242, 101 (1949).

[13]A. W. Weiss, Phys. Rev. 162, 71 (1967).

[14]C. Edmiston and M. Krauss, J. Chem. Phys. 45,
1833 (1966).

[15]P. L. Altick, Phys. Rev. 169, 21 (1968).

Calculations of Effusive-Flow Patterns. I. Knudsen-Cell Results*

B. P. Mathur and S. O. Colgate

*Molecular Beam Laboratory and the Department of Chemistry,
University of Florida, Gainesville, Florida* 32601

A simple and direct procedure has been used to calculate the flux gradients inside Knud-
sen cells and the related effusive-flow patterns. Knudsen cells of simple geometries with
knife-edge orifices and flat sources are considered. The calculated value of the Motzfeldt
factor (1.020) is in very good agreement with the literature value (1.020) and the Monte Carlo
calculations (1.020) for a cell of reduced height $H = 4.0$ and the knife-edge orifice of reduced
diameter $= 0.1064$. It is suggested that an extension of these calculations has an importance
in solving some of the problems encountered in determining the absolute total scattering cross
section from scattering measurements.

INTRODUCTION

The statistics of molecular dynamics and spatial
distribution for gases at equilibrium are well un-
derstood. Experiments with gases, however, often
involve mass flows having non-Maxwellian distri-
butions which, depending on the magnitudes and di-
rections of the gradients, are more or less diffi-
cult to characterize. The internal geometry of the
apparatus influences the details of mass-flow dis-
tributions. The effects of orifice shapes, in par-
ticular, on such distributions have been widely
studied for all types of flows from free molecular
effusions to supersonic jets. Generally, less at-
tention has been given to the effects of over-all
apparatus geometry including the location of tubu-
lations, chamber walls, and internal structures on
flow characteristics. At high pressures the con-
ducting apertures and channels have the greatest
influence on gas-flow patterns, but at low pres-
sures the arrangement of other fixed surfaces be-
comes increasingly important, and when gas mole-

cules collide with apparatus surfaces more fre-
quently than with other molecules in the vapor
phase the flow pattern is very sensitive to the de-
tailed arrangement of those surfaces.

The latter situation arises in effusive flows, and
any adequate description of flow patterns and den-
sity gradients in these cases will depend on the
over-all geometry of the flow system and not just
that of the apertures. Obtaining such descrip-
tions by straightforward solution of Boltzmann's
integrodifferential equation or Maxwell's equation
of change with explicit inclusion of gas-surface in-
teractions would be very difficult, but indirect
methods are more or less practical depending on
the complexity of the system. These methods are
substantially simplified if gas reflection by the
fixed surfaces is assumed to be diffuse since such
reflection momentarily restores certain equilib-
rium conditions to the molecular stream reflected
from a surface element.

Most treatments of effusive flow have used this
simplification since the classic work of Clausing[1]

on flow through finite channels. Since then, various workers[2] have extended the treatment in a direct way to include the over-all geometry of cylindrical Knudsen cells. The results of the Monte Carlo calculations of Ward *et al.* give details in general agreement with experiment and show clearly the significant effects of geometric irregularities within the cell such as occur when ceramic liners are used.

We have been interested in determining details of effusive-flow characteristics in molecular beam scattering chambers and have begun developing techniques to obtain them by both calculation and experiment. The calculation procedure is straightforward, at least for simple cell geometries. Since the method involves gas dynamics which are the same as those assumed in Ward's work, it was decided to use that work as a standard for testing the present scheme. Results of those tests are reported here; results for scattering chambers will be reported later.

FORMULATION AND CALCULATIONS

Consider the case of a rarefield gas, confined in a given volume where gas-phase collisions are practically negligible compared to molecular impacts on the walls, and where the walls reflect molecules diffusely according to the cosine law. In both molecular beam scattering experiments and Knudsen-cell effusive studies, the first condition is generally satisfied since mean free paths are usually long compared to chamber dimensions. Compliance with the second condition is more difficult to establish with general confidence, but at room temperatures and below, the reflection mechanism may be considered to involve an intermediate step of temporary adsorption on the walls and subsequent evaporation whereby the memory of the incident direction is lost. Reflection from a molecularly rough surface subject to these two conditions would typically exhibit a cosine-law distribution. The contribution to the local number density near a point P in the body of a gas by molecules reflected from surface element ds on a wall is[3]

$$dn = n_s(d\omega/4\pi) , \qquad (1)$$

where $d\omega$ is the solid angle subtended at P by the surface element in question and n_s is the effective equilibrium gas density at which the element appears to reflect. The total number density at P is found by integrating the above equation over all of the walls exposed to P, i.e.,

$$n_p = \tfrac{1}{4}\pi \int n_s d\omega . \qquad (2)$$

Here we have used this theorem to calculate the effective level of the radiative density inside a flat source Knudsen cell with knife-edge orifice. We have also calculated the Motzfeldt factor and determined the radial distribution of the effusive intensity through the orifice. We define the following geometrical dimensions, reduced in terms of the cell radius: H is the height of the cell; the radius of the cell is 1.0; and ρ is the radius of the aperture in the lid of negligible thickness (knife-edge orifice). Let α be the gross condensation coefficient[4] (the Langmuir coefficient, i.e., the probability that a vapor molecule condenses when striking the source), and γ the reflection coefficient (the probability that a vapor molecule will be reflected after collision with the cell walls). Further, let the height of the cell be divided into N cylindrical bands each of reduced bandwidth H/N; divide the lid into M circular rings with the reduced width $(1-\rho)/M$; and divide the source into M circular rings of reduced width $(1-\rho)/M$ and the central ring of radius equal to that of the orifice. Let the cylindrical bands be numbered in order starting from the source, and the circular rings on the source and on the lid numbered from the center outwards. Now, the procedure to calculate the steady-state conditions in such cells involves the following basic steps:

(i) Choose trial values for the apparent equilibrium-gas number densities n_i characteristic of the intensities of diffuse reflection from each of the various surface elements.

(ii) Calculate the total flux of molecules, Γ_i, incident on each surface element assuming the intensity of diffuse reflection from each such element to be uniform over its surface and neglecting gas-phase collisions.

(iii) Replace the trial values of n_i with those obtained by requiring the rates of reflection from the surface elements to be equal to the rates of molecular incidence on them diminished by the appropriate factors to account for condensation if any, i.e.,

$$\tfrac{1}{4}n_i\bar{v} = \gamma\Gamma_i \quad \text{or} \quad (1-\alpha)\Gamma_i + \tfrac{1}{4}n_0\bar{v}\alpha , \qquad (3)$$

where $\bar{v}$ is the average molecular speed. The first relation is to be used for surface elements on the cell walls and the second for those on the source.

(iv) The process is continued by iteration, calculating new values for Γ_i and n_i until suitable convergence is achieved.

The derivation of all of the equations required to permit the calculations of the Γ_i's is lengthy and will not be presented here. However, the salient features of the derivation are illustrated by considering a series of representative steps. For example, consider the molecules that strike an area ds located at P on the cylinder wall after reflection from the area ds' located elsewhere on that wall (see Fig. 1). These contribute to the molecular flux Γ_p on ds the amount
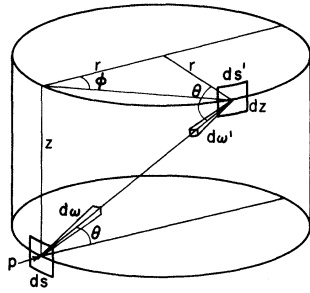
FIG. 1. Geometrical relationship between symbols used to compute the contribution to the flux on one cylindrical band caused by molecular reflection from another such band.

$$dΓ_p = (n'v/4π)\cos θ \, dω , \qquad (4)$$

where n' is the effective radiative density near ds' and is assumed to be uniform by cell symmetry around the wall at constant z (Fig. 1). Substituting for $\cos θ$ and the solid angle $dω$ the expressions in terms of the cell geometry in Eq. (4), and then integrating over the finite limits of $θ$ and z, we can write for the contribution to the total flux onto ds due to reflection anywhere from a finite cylindrical band of width $Δz$ at distance z from ds,

$$ΔΓ_p ≃ n' \frac{\overline{v}}{4} \left(K - \frac{2K^2 + 1}{2(K^2 + 1)^{1/2}} \right)_{K_1}^{K_2} , \qquad (5)$$

where

$$K = Z/2r .$$

The $≃$ sign is used here to emphasize the approximation resulting from assuming n' to be uniform over the band of finite height; the quality of the expression may be controlled by adjusting the magnitude of the arbitrary bands. Equation (5) represents the average flux over one cylindrical band due to reflection from another at a distance z (or from the same band, $z = 0$). It should be noted that n' is not the same as the actual number density near the band surface. The actual local densities can be calculated using Eq. (2) once the effective radiative densities are known, and further it can be shown that the gas has a mass motion resulting in a net creep toward the aperture as expected.

Other contributions to the net fluxes on the surface elements inside the cell are determined by methods analogous to that outlined above for the cylinder-wall–to–cylinder-wall case. The resulting expressions are: for the flux onto the cylinder wall from a flat ring on source (or lid) [see Fig. 2(a)],

$$ΔΓ = n' \frac{\overline{v}}{4} \left(\frac{K(1 + K^2 + R^2)}{[R^4 + 2R^2(K^2 - 1) + (K^2 + 1)^2]^{1/2}} \right)_{R_1}^{R_2} ; \qquad (6)$$

for the flux from a circular band on the cylinder wall to an element on the source (or lid) [see Fig. 2(b)],

$$ΔΓ = n' \frac{\overline{v}}{4} \left(\frac{1 - R^2 - K^2}{[(1 - R^2)^2 + 2K^2(1 + R)^2 + K^4]^{1/2}} \right)_{K_2}^{K_1} ; \qquad (7)$$

and for the flux from a flat ring on the source (or lid) to an element on the lid (or source) [see Fig. 2(c)],

$$ΔΓ = n' \frac{\overline{v}}{4} \left(\frac{R^2 - H^2 - R'^2}{[(H^2 + R'^2 + R^2)^2 - 4R'^2 R^2]^{1/2}} \right)_{R_1}^{R_2} . \qquad (8)$$

These equations permit the calculation of the total average incident fluxes on all of the various surface elements previously described. For the ith cylindrical band on the cell wall, for example, the total incident flux is

$$Γ_i = \sum_{j=1}^{N} ΔΓ_{ij} + \sum_{l=1}^{M} ΔΓ_{il} + \sum_{k=1}^{M+1} ΔΓ_{ik} , \qquad (9)$$

where $ΔΓ_{ij}$, $ΔΓ_{il}$, and $ΔΓ_{ik}$ give the flux contributions onto band i due to the jth cylindrical band, the lth lid ring, and the kth source ring, respectively. Similar expressions give the fluxes on the lid and source rings. After obtaining these fluxes, Eq. (3) is used to determine new values of the effective radiative densities. The cyclic iteration process is continued until the convergence is satisfactory.
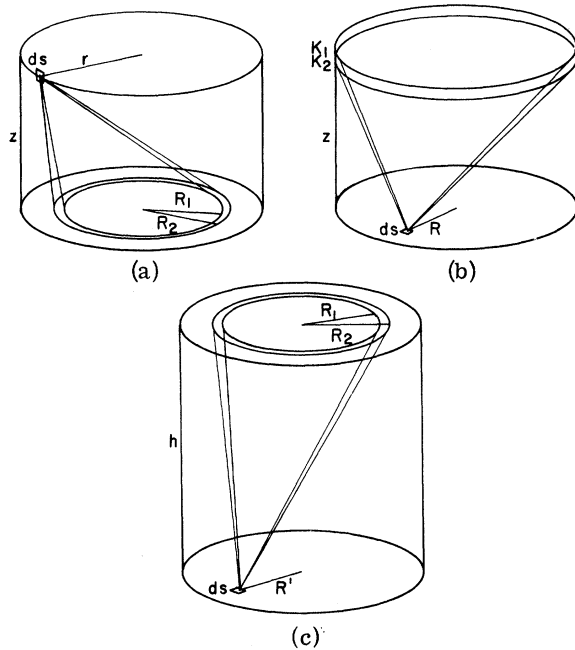

FIG. 2. Mathematical geometries and notations used to evaluate the incident fluxes on (a) a cylindrical band due to reflection from a flat ring, (b) a flat ring due to a cylindrical band, and (c) a flat ring due to another ring at the opposite end of the cell. $K = z/2r$.
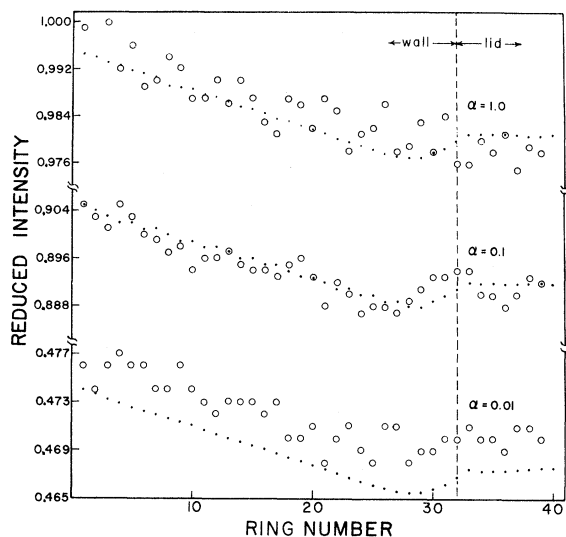
FIG. 3. Reduced–radiative–intensity curves for the inside of the cell A for different values of α and for $\gamma = 1.0$. The dots are the presently calculated values, and the open circles represent the Monte Carlo values taken from the data of Ward and Fraser (Ref. 9).

It may be pointed out that the relative density distribution is temperature independent so long as the temperature is uniform and constant over the cell walls. The effective radiative densities, reduced in terms of the equilibrium closed–cell density, thus obtained for three cell geometries are shown in Figs. 3–6.

Once we have the flux distributions or the levels of radiation inside the cell it is simple to calculate the effusive intensity. The angular distribution of the reduced effusive intensity according to the cosine law and that due to the theorem are given
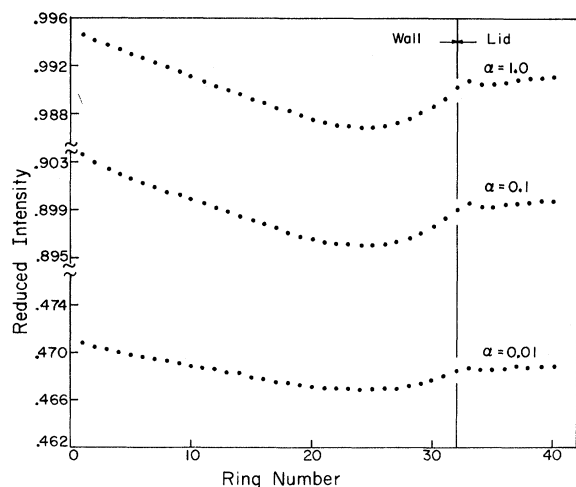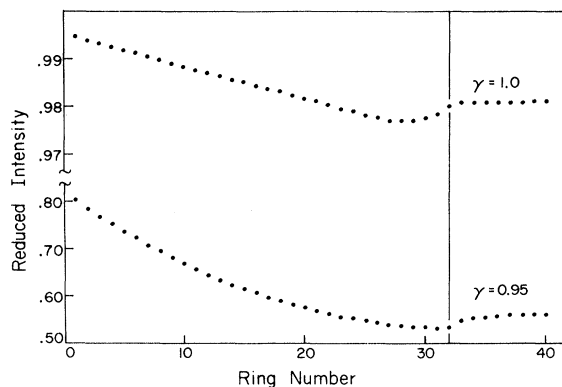

FIG. 5. Reduced–radiative–intensity curves for cell A with different wall and lid loss probabilities $(\alpha = 1.0)$.

in Tables I and II (only two such tables are given here in order to conserve the length of the article).

Calculation of the Motzfeldt Factor

According to the simplified treatment of the Knudsen cell, Motzfeldt[5] has given an expression relating the measured pressure (p_m) and the equilibrium pressure (p_e) in effusive systems. This relation in terms of the cell geometry and other constants is

$$f = 1 + \beta W_0 (1/\alpha + 1/W - 2) , \qquad (10)$$

where β is the reduced area of the orifice (orifice area/source area) W and W_0 are the Clausing transmission coefficients of the cell and the orifice, respectively, and f is generally called the Motzfeldt factor. For a knife–edge orifice, $W_0 = 1$. Using DeMarcus's[6] tables for W, the calculated values of f are given in Table III. Using the radia-

FIG. 4. Legend is same as in Fig. 3, except only our calculated values for the cell B are shown.
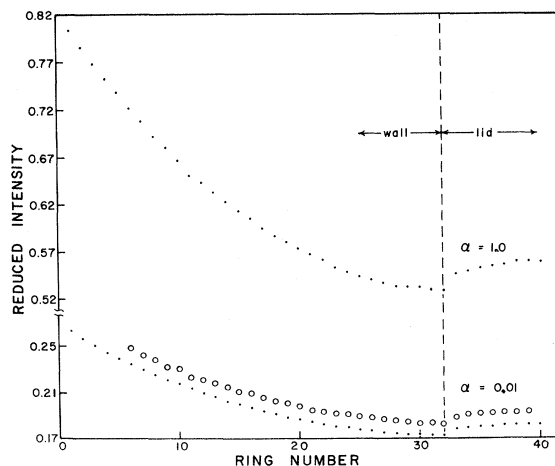

FIG. 6. Reduced–radiative–intensity curves for cell C for different values of α (taking $\gamma = 0.95$). The solid dots represent the present calculated values, and the open circles the Monte Carlo values of Ward et al.

TABLE I. Angular distribution of the reduced effusive intensity I_θ as a function of α for cell A and $\gamma = 1.0$.

Angle (deg)	Cosine law	I_θ Calculated $\alpha = 1.0$	$\alpha = 0.1$	$\alpha = 0.01$
0.0	1.0000	1.0000	1.0000	1.0000
2.3	0.9991	0.9991	0.9992	0.9992
3.9	0.9976	0.9976	0.9978	0.9978
5.5	0.9953	0.9953	0.9956	0.9956
7.0	0.9923	0.9923	0.9928	0.9928
8.6	0.9886	0.9886	0.9893	0.9894
10.2	0.9841	0.9841	0.9852	0.9853
11.7	0.9790	0.9790	0.9805	0.9807
13.2	0.9732	0.9732	0.9754	0.9757
14.2	0.9692	0.9639	0.9654	0.9655
14.6	0.9672	0.9613	0.9625	0.9626
15.1	0.9651	0.9586	0.9597	0.9597
15.6	0.9627	0.9556	0.9567	0.9567
16.2	0.9601	0.9524	0.9536	0.9536
16.7	0.9573	0.9489	0.9499	0.9499
17.4	0.9541	0.9451	0.9461	0.9461
18.0	0.9506	0.9409	0.9420	0.9420
18.7	0.9466	0.9364	0.9374	0.9374
19.5	0.9422	0.9314	0.9324	0.9324
20.4	0.9372	0.9528	0.9269	0.9269
21.3	0.9315	0.9196	0.9207	0.9207
22.3	0.9251	0.9127	0.9137	0.9137
23.3	0.9178	0.9049	0.9059	0.9059
24.5	0.9094	0.8960	0.8970	0.8970
25.8	0.8998	0.8859	0.8869	0.8869
27.2	0.8886	0.8742	0.8752	0.8752
28.8	0.8755	0.8608	0.8618	0.8618
30.6	0.8602	0.8452	0.8462	0.8461
32.6	0.8422	0.8269	0.8279	0.8278
34.8	0.8209	0.8056	0.8063	0.8063
37.3	0.7954	0.7798	0.7807	0.7807
40.1	0.7649	0.7493	0.7502	0.7502
43.2	0.7282	0.7129	0.7137	0.7137
46.8	0.6839	0.6691	0.6699	0.6699
50.9	0.6305	0.6165	0.6173	0.6172
55.4	0.5665	0.5536	0.5543	0.5543
60.6	0.4902	0.4790	0.4795	0.4795
66.3	0.4008	0.3916	0.3921	0.3921
72.6	0.2982	0.2916	0.2919	0.2919
79.3	0.1842	0.1803	0.1805	0.1805
86.4	0.0623	0.0611	0.0612	0.0612

tive flux gradients inside the cell, we can also calculate f values in three different ways:

(a) First, f values can be calculated by computing the effective density at the orifice (and estimating f as the ratio of this density to the equilibrium density n_0)

$$f = 2\pi \Big/ \left(\sum_{i=1}^{N} N_1(i)\Omega(i) + \sum_{k=1}^{M+1} N_2(k)\Omega'(k) \right), \quad (11)$$

where Ω and Ω' are, respectively, the solid angles subtended by the ith band [radiative density level $N_1(i)$] or the kth source cell [radiative density $N_2(k)$] at the center of the aperture. (b) Similarly,

f values can be calculated from the mass-balance equation, i.e.,

$$f = \pi R^2 (1 - \alpha) / \alpha \left(\sum_{k=1}^{M+1} A_k [1 - N_2(k)] \right), \quad (12)$$

where A_k is the reduced area of the kth source cell. (c) Third, f values can be calculated from the total flux through the aperture, i.e.,

$$f = (\pi R)^2 \Big/ \gamma \left(\sum_{i=1}^{N} N_1(i) B_i \omega(i) \cos\theta + \sum_{k=1}^{M+1} N_2(k) A_k \omega'(k) \cos\theta \right), \quad (13)$$

TABLE II. Angular distribution of the reduced effusive intensity I_θ as a function of α for cell B and $\gamma = 1.0$.

Angle (deg)	Cosine law	I_θ Calculated $\alpha = 1.0$	$\alpha = 0.1$	$\alpha = 0.01$
0.0	1.0000	1.0000	1.0000	1.0000
4.6	0.9967	0.9967	0.9968	0.9968
7.8	0.9907	0.9907	0.9909	0.9909
10.9	0.9819	0.9819	0.9823	0.9823
14.0	0.9704	0.9704	0.9710	0.9711
16.9	0.9566	0.9566	0.9575	0.9576
19.8	0.9408	0.9408	0.9420	0.9422
22.6	0.9232	0.9232	0.9249	0.9251
25.3	0.9043	0.9043	0.9067	0.9070
26.9	0.8916	0.8868	0.8884	0.8886
27.7	0.8855	0.8803	0.8818	0.8819
28.5	0.8790	0.8735	0.8748	0.8750
29.3	0.8720	0.8662	0.8674	0.8675
30.2	0.8643	0.8583	0.8594	0.8596
31.1	0.8561	0.8498	0.8509	0.8510
32.1	0.8471	0.8405	0.8416	0.8417
33.1	0.8373	0.8305	0.8315	0.8316
34.2	0.8266	0.8196	0.8206	0.8207
35.4	0.8150	0.8077	0.8087	0.8089
36.6	0.8022	0.7948	0.7958	0.7959
38.0	0.7883	0.7807	0.7817	0.7818
39.4	0.7731	0.7653	0.7663	0.7664
40.9	0.7564	0.7485	0.7494	0.7495
42.4	0.7380	0.7301	0.7310	0.7311
44.1	0.7179	0.7099	0.7108	0.7109
45.9	0.6958	0.6878	0.6887	0.6888
47.8	0.6715	0.6636	0.6644	0.6645
49.8	0.6449	0.6371	0.6378	0.6379
52.0	0.6156	0.6080	0.6087	0.6088
54.3	0.5836	0.5762	0.5770	0.5770
56.7	0.5487	0.5416	0.5423	0.5423
59.3	0.5105	0.5039	0.5045	0.5046
62.0	0.4691	0.4630	0.4636	0.4637
64.9	0.4244	0.4189	0.4194	0.4195
67.9	0.3764	0.3715	0.3720	0.3720
71.0	0.3251	0.3210	0.3214	0.3214
74.3	0.2707	0.2674	0.2677	0.2678
77.7	0.2137	0.2112	0.2114	0.2114
81.1	0.1544	0.1526	0.1528	0.1528
84.6	0.0933	0.0924	0.0925	0.0925
88.2	0.0312	0.0309	0.0310	0.0310

TABLE III. Motzfeldt factors (f) for knife-edge orifice Knudsen cells with zero wall and lid loss probability.

		Calculated values of f			
α	Eq. (7)	Eq. (8)	Eq. (9)	Eq.(10)	Monte Carlo (Ref. 9)
		Cell A	$W=0.3589$		
1.0	1.020	1.020	1.016	1.015	1.022
0.1	1.122	1.122	1.122	1.117	1.124
0.01	2.141	2.141	2.141	2.131	2.128
		Cell B	$W=0.5136$		
1.0	1.011	1.010	1.010	1.006	
0.1	1.113	1.113	1.108	1.108	
0.01	2.131	2.136	2.127	2.127	

where B_i is the reduced area of the ith cylindrical band, $\omega(i)$ and $\omega'(k)$ are the solid angles subtended at the midpoint of the ith band or kth cell by the orifice, respectively, and ϕ and θ are the angles of effusion measured from the normal through the center of the aperture. These values of f are also given in Table III.

It may be pointed out that there are some problems in determining the required solid angles appearing in the above equations. Except for the simplest cases, it is not always possible to express these angles in terms of ordinary fractions. Masket and Rogers[7] have tabulated values of solid angles subtended by circular disks and the lateral surfaces of right circular cylinders. Though these tables are exhaustive, it proved more convenient to compute the necessary solid angles generating required values of complete and incomplete elliptic integrals[8] from standard scientific subroutines available in the computer library.

RESULTS AND DISCUSSION

The present calculations were programed for two straight cylindrical cells of diameter 0.25 in., orifice diameter 0.0226 in., and heights 0.5 in. (cell A) and 0.25 in. (cell B). As mentioned earlier, we have limited the present calculations to knife-edge orifices (the orifice Clausing factor is equal to 1.0). The dimensions of cell A were taken to be the same as those of Ward and Fraser[9] to facilitate comparison of the present results with the Monte Carlo calculations. They have used the Monte Carlo technique to investigate similar flux relationships within Knudsen cells. Unfortunately, most of their data are presented graphically,[9] but we have tried to make the best use of it.

As mentioned earlier, the cell height is divided into 32 cylindrical bands, and the lid and source into eight circular rings plus the orifice (in the case of the lid) and the central ring (for the source). Assuming there are no wall and lid losses ($\gamma = 1.0$), the flux gradients for the inside of the two cells obtained by using the theorem are as shown in Figs. 3 and 4, respectively. Reduced flux intensities are plotted against ring numbers (henceforth numbered consecutively from the band nearest the source to the aperture). In Fig. 3 are also shown the data of Ref. 9 (these were obtained by photographically enlarging the published graph and reading the points from a coordinate overlay). In each figure, curves are plotted for three different values of α, 1.0, 0.1, and 0.01, respectively. As is evident from Fig. 3, our calculated values for cell A are in very good agreement with those of Ward and Fraser. The reason for the slight discrepancy for $\alpha = 0.01$ is not entirely understood. It may result from our assumption that diffuse reflection from a finite surface element is uniform over that surface, or it may involve errors in our rather crude method of obtaining the numerical values of Ward's data. The fact that a similar disparity is found in a cell of different magnitude (Fig. 6) suggests that the former or some other mathematical difference is likely the cause. At any rate, the effect is small and the over-all agreement is still good. Cell B also shows the same features lending further support to our way of calculation. These curves clearly show that in the steady state the flux distribution inside the cell is not the same everywhere.

Tables I and II are representative of the angular dependence of the reduced intensity of the effusive flux according to the cosine law and as calculated according to the theorem. Calculated values for cell A with three different values of α are given in Table I, and values for cell B are given in Table II. It will be seen that the calculated values are practically independent of α and are in good agreement with the cosine-law values except toward the lower end (large angles) of the spectrum λ, where the visible cell walls radiate at their lowest levels.

For cell A we also assumed a 0.5% wall and lid loss probability and then determined the flux distribution inside the cell for the case when $\alpha = 1$. These values are shown in Fig. 5, where the curve for $\gamma = 1.0$ is also given for comparison. These plots again show the same general features as shown by the Monte Carlo calculations. Figure 6 is again the same as Fig. 5, but for a third cell C of dimensions $H = 4.0$, $R = 0.124$, $W_0 = 1.0$, and $W = 0.3589$. Here the values are for $\gamma = 0.95$ and $\alpha = 1.0$ and 0.01. Again it will be noticed that there is good agreement in our values (solid dots) and the Monte Carlo values[9] (open circles), for $\alpha = 0.01$.

In Table III are given the values of the Motzfeldt factors calculated for cells A and B according to Eqs. (10)–(13). Also recorded are values for cell A from the Monte Carlo technique. As is evident, the agreement in each case is good (maximum difference < 1%). The internal consistency of the calculations is also good (~ 1%).

The present method produces less scatter than that characteristic of the Monte Carlo technique, and, therefore, shows sharper detail in the computed flux gradients. This is evident in Fig. 3. Since the contribution to the incident flux on a surface element due to a radiative source is proportional to the solid angle subtended by that source at the surface element, it follows that the net reduction in flux at the surface element below that characteristic of complete equlibrium (reduced intensity = 1) is related to the exposure of that element to any sinks (the aperture in this case). Moving along the cylindrical wall of the Knudsen cell from the source toward the lid, the solid angles $[\omega \sim A_a (\cos\theta)/x^2]$ subtended by the aperture increases if x^2 (x is the distance from the surface element to center of aperture, θ is the angle between x and the normal to the aperture, and A_a is the area of the aperture) decreases faster than $\cos\theta$; the angle then passes through a maximum where these two terms decrease at the same rate; and finally it decreases as the cosine term begins to fall off more rapidly. These considerations imply that the actual flux distributions should show a minimum corresponding the maximum exposure to the aperture. Such minima have been predicted[10,11] and are well defined by the present calculations, but they are less resolved by the Monte Carlo calculations[9] (see Fig. 3).

The exact location of the above minima cannot be expected to correspond with the location of maximum exposure to the aperture because of nonuniformity of the radiative flux. Substantial changes in α produce little effect on the position of the minimum (see Figs. 3 and 4). Small changes in γ, however, result in large shifts. This is evident in Fig. 5 where the minimum present at $\gamma = 1.0$ completely disappears when γ is reduced by 5%.

This is due to the fact that for $\gamma < 1$ the cell walls themselves become partial sinks and the exposure to these increases with increasing distance from the source. In Fig. 5 (note the different scales for the two curves) the monotonic decrease in reduced intensity from the source to the lid due to this effect at $\gamma = 0.95$ overshadows the lesser effect arising from variation in exposure to the aperture, and the corresponding minimum in the curve is not resolved. The rather abrupt increase in reduced intensity between the cylindrical wall and the flat lid is evident in all cases studied. This effect results from the marked change in exposure of a surface element to the source as its orientation with respect to the source is changed from perpendicular to parallel. This behavior is typical of effects produced by discontinuities in cell geometry, and such sudden changes in radiative flux densities produce irregularities in the patterns of effusive flow when the internal geometrical discontinuities are "visible" from outside the cell. Ward et al.[2] have observed these effects using cells with liners shorter than the cell heights.

The results presented above clearly indicate the importance of the theorem and the suggested procedure. The limited treatment of the simple cell can be easily extended to more complicated systems. Some work is in progress concerning molecular beam scattering chambers, the details of which will be published later. Experiments are also being carried out to give an indirect proof of the theorem.

ACKNOWLEDGMENTS

*Work supported in part by NASA.

[1]P. Clausing, Z. Physik 66, 471 (1931); J. Vac. Sci. Technol. 8, 636 (1971); see also W. E. DeMarcus, U.S. AEC Report No. K-1302, Part 1, 1956 (unpublished).

[2]C. J. Whitman, J. Chem. Phys. 20, 161 (1952); J. W. Ward, R. N. R. Mulford, and M. Kahn, ibid. 47, 1710 (1967); J. W. Ward, R. N. R. Mulford, and R. L. Bivins, ibid. 47, 1718 (1967); J. W. Ward, ibid. 47, 4030 (1967); 49, 5129 (1968); 50, 1877 (1969); B. R. Baker and B. J. Wood, J. Vac. Sci. Technol. 7, 206 (1970).

[3]S. O. Colgate, Vacuum 21, 483 (1971).

[4]I. N. Stranski and G. Wolf, Research (London) 4, 15 (1951); L. Brewer and J. S. Kane, J. Phys. Chem. 49, 105 (1955); G. N. Winslow, in Condensation and Evaporation of Solids, edited by E. Rutner, P. Goldfinger, and J. P. Hirth (Gordon and Breach, New York, 1964); An. N. Nesmeyanov, Vapour Pressures of the Elements (Academic, New York, 1963).

[5]K. Motzfeldt, J. Phys. Chem. 59, 139 (1955).

[6]W. C. DeMarcus, U. S. AEC Report No. K-1302, 1957, Part 3 (unpublished).

[7]A. V. H. Masket and W. E. Rodgers, Tables of Solid Angles (North Carolina U. P., Chapel Hill, N. C., 1962); see also A. V. H. Masket, Rev. Sci. Instr. 28, 191 (1957); F. Paxton, ibid. 30, 254 (1959); A. V. H. Masket, R. L. Macklin, and H. W. Schmitt, ibid. 28, 189 (1957).

[8]P. F. Byrd and M. D. Friedman, Handbook of Elliptic Integrals for Engineers and Physicists (Springer-Verlag, Berlin, 1956); Handbook of Mathematical Functions with Formulas, Graphs. and Mathematical Tables, edited by M. Abramowitz and I. A. Stegun, Natl. Bur. Std. Appl. Math. Ser. 55 (U.S. GPO, Washington, D. C., 1965).

[9]J. W. Ward and M. V. Fraser, J. Chem. Phys. 49, 3743 (1968).

[10]E. W. Balson, J. Phys. Chem. 65, 1151 (1961).

[11]K. D. Carlson, P. W. Gilles, and R. J. Thorn, J. Chem. Phys. 38, 2064 (1963).